

1 **Updated atmospheric speciated mercury emissions from**
2 **iron and steel production in China during 2000-2015**

3 **Qingru Wu^{1,2}, Wei Gao^{1,2}, Shuxiao Wang^{1,2*}, Jiming Hao^{1,2}**

4 ¹School of Environment, and State Key Joint Laboratory of Environment Simulation and
5 Pollution Control, Tsinghua University, Beijing 100084, China

6 ²State Environmental Protection Key Laboratory of Sources and Control of Air Pollution
7 Complex, Beijing 100084, China

8 *Correspondence to:* S. X. Wang (shxwang@tsinghua.edu.cn)

9 **Abstract**

10 Iron and steel production (ISP) is one of the significant atmospheric Hg emission sources
11 in China. Atmospheric mercury (Hg) emissions from ISP during 2000-2015 were estimated by
12 using a technology-based emission factor method. To support the application of this method,
13 databases of Hg concentrations in raw materials, technology development trends, and Hg
14 removal efficiencies of air pollution control devices (APCDs) were constructed through
15 national sampling and literature review. Hg input to ISP increased from 21.6 t in 2000 to 94.5
16 t in 2015. In the various types of raw materials, coking coal and iron concentrates contributed
17 35%-46% and 25%-32% of the total Hg input. Atmospheric Hg emissions from ISP increased
18 from 11.5 t in 2000 to 32.7 t in 2015 with the peak of 35.6 t in 2013. Pollution control
19 promoted the increase of average Hg removal efficiency, from 47% in 2000 to 65% in 2015.
20 During the study period, sinter/pellet plant and blast furnace were the largest two emission
21 processes. However, emissions from roasting plant and coke oven cannot be ignored, which
22 accounted for 22%-34% of ISP's emissions. Overall Hg speciation shifted from 50/44/6
23 (gaseous elemental Hg (Hg^0) / gaseous oxidized Hg (Hg^{II}) / particulate-bound Hg (Hg_p)) in
24 2000 to 40/59/1 in 2015, which indicated higher proportion of Hg deposition around the
25 emission points. Future emissions of ISP were expected to decrease based on the
26 comprehensive consideration crude steel production, steel scrap utilization, energy saving,
27 and pollution control measures.

28

29 **1 Introduction**

30 China is the largest iron and steel production (ISP) country in the world. Crude steel
31 production has increased from 127 Mt in 2000 to 804 Mt in 2015 (CISIA, 2001-2016). Rapid
32 economic development has led to large emissions of air pollutants including mercury (Hg)
33 emissions of ISP (Liu et al., 2016; Wang K. et al., 2016; Wang et al., 2014). To reduce Hg
34 pollution, it is important to quantify atmospheric Hg emissions from ISP.

35 According to existing national inventories, atmospheric Hg emissions from ISP
36 increased from 4.9 t in 1999 to 25.5 t in 2010 (AMAP/UNEP, 2008; Streets et al., 2005; Wu et
37 al., 2006; Zhang et al., 2015a). In these studies, Hg emissions were determined as the product
38 of crude steel production and unique emission factor of 0.04 g/t steel produced which did not
39 consider the emissions from roasting plant and coke oven (two processes of ISP). However,
40 field experiments in China's ISP indicated that these two processes are significant for Hg
41 emissions. Emissions from coke oven accounted for 17%-49% of the total Hg emissions of
42 ISP (Wang F. Y. et al., 2016). Thus, these two processes are potentially important in shaping
43 the trends of ISP Hg emissions. Later long-term emission inventories revised the unique
44 emission factor with dynamic factors by adopting transformed normal distribution function
45 (Tian et al., 2015; Wang K. et al., 2016; Wu et al., 2016). Such method was based on the
46 assumption that the emission factor was gradually improved according to the simulation curve
47 and attempted to simulate the impact of technology improvement and pollution control on
48 emission factor variation. However, the emission factors actually did not link with technology
49 and APCDs directly. Thus, the simulated emission factors may be quite different from actual
50 situation during a certain period (e.g. ten years) when technology and APCDs experienced
51 dramatic change (Wu et al., 2016), especially under the background of tightening requirement
52 of environmental protection in China in the past decades (MEP, 2011; NEA, 2014; SC, 2013).
53 Recent global Hg assessment report applied a technology-based emission factor method to
54 estimate the emissions of global ISP including China's (AMAP/UNEP, 2013). However, most
55 of the parameters were from developed countries, which may impact the accuracy of
56 emissions from developing countries such as China. In addition, emissions from roasting
57 plants and arc steel making process (using scrap to produce steel) were not calculated in the

58 report.

59 The dominant parameters of a technology-based emission factor included Hg removal
60 efficiencies of APCDs and Hg concentrations in raw materials (Wu et al., 2016; Wu et al.,
61 2012; Zhang et al., 2015a). As to Hg removal efficiencies of APCDs, we hypothesized that the
62 use of data from recent field experiments on atmospheric Hg emission characteristics in
63 China's ISP will provide a foundation for the technology-based emission factor model (Wu et
64 al., 2016; Wu et al., 2012; Zhang et al., 2015a). However, current studies cannot support the
65 construction of Hg concentration databases for raw materials. Various raw materials were
66 used in ISP, covering iron concentrates, iron block, alloy materials, steel scrap, coal, and
67 additives (mainly limestone and dolomite). Field experiments in three China's steel smelters
68 indicated that the concentrations of iron concentrates were in the range of 23-66 ng/g (Wang
69 F.Y. et al., 2016; Zhang et al., 2015b). However, the Hg concentration data from limited
70 samples may lead to large uncertainty of the national inventory. Many studies have reported
71 Hg concentrations in coal (Swaine, 1992; Tian et al., 2010; USGS, 2004; Zhang et al., 2012).
72 But the specific requirement of low-sulfide coal (less than 1.2%) in ISP may lead to different
73 Hg concentrations in the consumed coal (Tao and Wang, 1994), since low-sulfide coal was
74 generally accompanied by low-Hg (Zhang, 2012). Rare studies have reported Hg concentrations
75 in steel scrap and dolomite. Therefore, constructing Hg concentration databases of raw
76 materials was the base to apply a technology-based emission factor model for China's ISP.

77 In this study, a technology-based emission factor model was constructed to estimate
78 atmospheric Hg emissions from China's ISP. To fulfill this aim, raw materials consumed in
79 steel smelters have been sampled and Hg concentrations have been analyzed to construct the
80 Hg concentration databases. Up-to-date Hg removal efficiencies from field experiments and
81 the development trends of production technology and APCDs have been summarized to
82 support the application of emission factor model.

83 **2 Methodology**

84 **2.1 Technology-based emission factor model for ISP**

85 Generally speaking, ISP method included long process steel making method and short

86 process steel making method. The long process steel making method included roasting plant,
 87 coke oven, sinter/pellet plant, blast furnace, and oxygen steel making (**Fig. 1**). The short
 88 process steel making method produced crude steel mainly from steel scrap in arc steel making
 89 process directly.

90 Thus, atmospheric Hg emissions from ISP by province can be calculated as follows.

$$\begin{aligned}
 E_i(t) &= E_{i,l}(t) + E_{i,s}(t) \\
 &= E_{i,l,r}(t) + E_{i,l,c}(t) + E_{i,l,p}(t) + E_{i,l,b}(t) + E_{i,l,o}(t) \\
 &\quad + E_{i,s,a}(t)
 \end{aligned} \tag{E1}$$

91 where, E was atmospheric Hg emissions from ISP, t; i was province; t referred to studied
 92 year; l and s referred to long and short process steel making method; r, c, p, b, o, a referred to
 93 roasting plant, coke oven, sinter/pellet plant, blast furnace, oxygen steel making, and arc steel
 94 making.

95 For each process x , the technology-based emission factor and speciated Hg emissions
 96 can be calculated as follows.

$$EF_{i,x,k}(t) = \sum_j C_{i,x,j} \times M_{i,x,j}(t) \times S_i(t)^{-1} \times \gamma_x \times \sum_m \theta_m(t) \times \delta_{k,m} \times (1 - \eta_m) \times 1000^{-1} \tag{E2}$$

$$E_{i,x,k}(t) = EF_{i,x,k}(t) \times S_i(t) \tag{E3}$$

97 where, EF was emission factor, g/t; x was studied process; k was speciated Hg; j was the
 98 type of consumed raw material; C was Hg concentration in the consumed raw material, ng/g
 99 (see section 2.2.1); M was the consumption of raw material, Mt (see section 2.2.2); S was the
 100 production of crude steel, Mt (see section 2.2.2). γ was Hg release rate, which meant the
 101 percentage of Hg released to flue gas from raw material, %. Hg release rate were collected
 102 from field experiment studies (**Table S1**). That was 98% for roasting plant, 80% for coke
 103 oven, 85% for sinter/pellet plant, 98% for blast furnace, 80% for oxygen steel making furnace,
 104 and 95% for arc steel making furnace. m referred to the type of APCD combination (see
 105 section 2.2.3); δ was the proportion of different Hg speciation (see section 2.2.3), %; θ was
 106 the application rate of different APCD combinations (see section 2.2.3), %; η was Hg removal
 107 efficiency (see section 2.2.3), %.

108 2.2 Parameters for model

109 2.2.1 Hg concentrations in raw materials

110 For the long process steel making method, the dominant raw materials included iron
111 concentrates, iron block, coal, limestone, dolomite, alloy, and steel scrap (**Fig. 1**). In the
112 roasting plant, limestone and dolomite were roasted together or separately to make quick lime
113 and caustic dolomite. In the coke oven, washed coal was used to produce coke. In the
114 sinter/pellet plant, iron-containing materials (mainly iron concentrates), quick lime, caustic
115 dolomite, and produced coke (mainly coke breeze) were mixed to produce sintered/pellet
116 block, which were used as raw materials with coal and produced coke in the blast furnace.
117 The produced pig iron from blast furnace and additional scraps were used to produce steel in
118 the oxygen steel making processes. For the short process steel making method, arc steel
119 making process was applied to produce steel by mainly using scraps as raw materials. In each
120 process, Hg input due to the use of intermediated products (e.g., quick lime, caustic dolomite,
121 and coke) was calculated by using mass balance method (Wu et al., 2012).

122 National sampling and Hg concentration analysis were conducted to construct the Hg
123 concentration databases for the consumed raw materials. The sampling, preparation and
124 analysis methods were described in detail in our previous studies (Wu et al., 2012; Zhang et
125 al., 2012). Lumex 915M + pyro attachment (with a detection limit of 0.5 ng/g) was applied to
126 analyze Hg concentration by using U.S. EPA Method 7473 (US EPA, 1998). Number of
127 samples and Hg concentrations in dominant raw materials by province were shown in **Table 1**.
128 National Hg concentrations (median value) in the consumed iron ores were 20 (0.6-387) ng/g,
129 which were lower than the median value of 30 (0.6-600) ng/g used in the global assessment
130 report (AMAP/UNEP, 2013). Overall Hg concentrations in the consumed coking coal (82
131 ng/g) and pulverized coal injection (PCI) coal (73 ng/g) were lower than the 170 (8-2248)
132 ng/g (Zhang, 2012) used in China's coal combustion sectors but higher than the 55 (50-60)
133 ng/g of global assessment report. Hg concentrations in the limestone were 18 (0.9-2753) ng/g.
134 Although the median value was lower than value of 30 (20-50) ng/g applied in the global
135 assessment report, the variation range was much wider according to our analysis. Hg
136 concentrations (median value) in the dolomite and iron block were 9 ng/g and 19 ng/g. In

137 oxygen and arc steel making processes, the main iron-containing materials were steel scrap,
138 alloy scrap, and pig iron. Hg concentrations (median value) in steel scrap and alloy scrap were
139 48 and 2 ng/g while the concentrations in pig iron were less than detection limit. For province
140 with samples no less than 15, the distribution characteristics of Hg concentrations of the
141 samples were generated by using the batch fit function of Crystalball software. Otherwise, Hg
142 concentrations were assumed to fit normal distribution.

143 2.2.2 Provincial consumptions of raw materials

144 Provincial consumptions of raw materials in 2015 were shown in **Table S2**. National
145 limestone consumptions were converted from quick lime consumptions (Ma, 2011) by using
146 the factor of 1.95 t limestone to produce 1 t quick lime (CISIA, 2001-2016) (**Table S3**).
147 National dolomite consumptions were derived from China steel statistics report (Ma, 1995)
148 according to the production trends of crude steel. The limestone and dolomite can be
149 consumed in the roasting and sinter/pellet plant. In the sinter/pellet plants, additives
150 (including limestone and dolomite) consumptions were approximately 153.9 kg/t sinter
151 produced or 10.5 kg/t pellet produced (CISIA, 2001-2016). We assumed that 88% of the
152 additives were limestone and 12% were dolomite according to field experiments (Wang F. Y.
153 et al., 2016). The rest of limestone and dolomite were consumed in the roasting plants.
154 Provincial consumptions of limestone and dolomite were distributed according to the
155 proportions of provincial pig iron productions in national production (Table S2). Provincial
156 pig iron productions were collected directly from yearbooks (CISIA, 2001-2016).

157 Provincial coking coal consumptions were converted from provincial coke consumptions
158 (CISIA, 2001-2016). Generally, there were two main types of coke production methods,
159 including machining coke production method and indigenous coke production method. Coal
160 consumptions were 1.35 t to produce 1 t of machining coke or 1.65 t to produce 1 t of
161 indigenous coke (UNEP, 2013; Wang, 1991). The produced cokes were used as raw materials
162 in both sinter/pellet plant and blast furnace. Provincial coke consumptions in blast furnace
163 were converted according coke ratio of 363-388 kg coke per t pig iron produced (CISIA,
164 2001-2016). The rest of cokes were assumed to be consumed in sinter/pellet plant.

165 National iron concentrate consumptions were converted from sinter/pellet productions.

166 Approximately 0.91-0.92 t and 0.96-0.97 t of iron concentrates were needed to produce 1 t
167 sinter and 1 t pellet, respectively (CISIA, 2001-2016). National sinter and pellet productions
168 were obtained directly from yearbooks (CISIA, 2001-2016) and provincial data were
169 converted according to provincial pig iron productions.

170 National PCI coal consumptions in blast furnace were collected from national energy
171 statistical yearbook (NESA, 2001-2016) and the provincial data were converted according to
172 provincial pig iron productions. The iron block consumption in blast furnace were converted
173 from pig iron production by using the factor of 156 kg iron block per t pig iron produced
174 (CISIA, 2001-2016).

175 The steel scrap was consumed in both oxygen and arc steel making process.
176 Consumptions of steel scrap in oxygen and arc steel making process were approximately 59.4
177 and 361.9 kg/t crude steel produced. Alloy consumptions to produce per t crude steel were
178 16-17 kg in oxygen steel making process and 140-156 kg in arc oxygen making process.
179 Oxygen and arc steel productions were collected directly from yearbooks (CISIA, 2001-2016).
180 Based on these ratios, provincial steel scrap and alloy consumptions were converted from
181 provincial crude steel productions.

182 2.2.3 Application rate, Hg removal efficiency, and Hg speciation

183 In the roasting plant, blast furnace, and steel making process, dust collectors such as
184 venturi, cyclone (CYC), wet scrubber (WS), electrostatic precipitator (ESP), and fabric filter
185 (FF) were used for flue gas dedusting. In coke oven process, washed coal were consumed and
186 the flue gas was cleaned with dust collectors or with additional washing scrubbers. For flue
187 gas from sinter/pellet plant, they were generally cleaned with dust collectors. Additional flue
188 gas desulfurization towers (FGD) were gradually applied after 2010. It should be noted that
189 the flue gas after dust collectors were generally collected as coal gas in gasometer. However,
190 rare APCDs were applied during the coal gas usage process. Thus, we assumed that all Hg in
191 the coal gas was emitted to air. The application rates of different APCD combinations by
192 process during 2005-2010 were collected from previous studies (Wang et al., 2014; Zhao et
193 al., 2013). The data of 2000-2004 and 2011-2015 were mainly derived from yearbooks
194 (CISIA, 2001-2016; NBS, 2001-2016) (Table S4). Hg removal efficiencies and speciation

195 profiles of APCDs (**Table S4**) were collected from field experiments and literature on
196 emission studies (Gao, 2016; Wang F. Y. et al., 2016; Zhang et al., 2015b). The distribution
197 characteristics of Hg removal efficiencies were assumed to fit normal distribution
198 characteristics.

199 **2.3 Uncertainty analysis**

200 Monte Carlo simulation was introduced to estimate the uncertainty of emissions.
201 Detailed description of the simulation processes has been reported in our previous studies
202 (Hui et al., 2016; Wu et al., 2016; Zhang et al., 2015a). In this study, the (P50-P10)/P50 and
203 (P90-P50)/P50 values were still regarded as lower and upper limits of uncertainties with 80%
204 confidence degree, where P10, P50, and P90 meant that the probabilities of actual results
205 lower than corresponding values were 10%, 50%, and 90%, respectively.

206 **3 Results and Discussion**

207 **3.1 Hg input trends**

208 Hg input to ISP increased from 21.6 t in 2000 to 94.5 t in 2015 (**Fig. 2**). The peak of Hg
209 input was in 2014 when the crude steel production reached the highest value (**Table S3**).
210 During 2000-2014, the average annual growth rate (AAGR) of Hg input was 11% while Hg
211 input reduced by 3% from 2014 to 2015. In the various types of raw materials, coking coal
212 and iron concentrates contributed the largest amount of Hg input, accounting for 35%-46%
213 and 25%-32% of the total, respectively. Hg input due to the use of coking coal increased from
214 9.9 t in 2000 to 33.5 t in 2015. Hg input with iron concentrates increased at AAGR of 12%
215 from 2000 and reached 29.2 t in 2015. The PCI coal brought approximately 6%-9% of Hg to
216 ISP. Hg in the additives (including limestone and dolomite) contributed 12%-18% of total Hg
217 input. Hg in the iron block was in the range of 0.6-3.6 t. Hg input due to the use of steel scrap
218 and alloy was 4.1 t in 2015, accounting for 4% of national total. However, steel scrap and
219 alloy contributed 7% of total crude steel production in 2015 (CISIA, 2016).

220 3.2 Hg emission trends

221 3.2.1 Hg emission trends by process

222 Atmospheric Hg emissions from ISP increased from 11.5 t in 2000 to 32.7 t in 2015 (**Fig.**
223 **3**). The peak of emissions was in 2013 when the emissions reached 35.6 t. In 2015, emissions
224 from long process steel making method and short process steel making were 32.2 t and 0.5 t,
225 accounting for 98.3% and 1.7% of national total, respectively. Thus, emissions from long
226 process steel making were still the dominant emission process of China's ISP. Among the
227 processes, emissions from sinter/pellet plant accounted for 42%-49% of annual total. Its
228 emissions increased from 4.8 t in 2000 at the AAGR of 10.1% and reached 15.9 t in 2015.
229 Blast furnace was also significant Hg emission process. Its emissions increased from 1.9 t in
230 2000 to 7.9 t in 2015 at AAGR of 10.0%. AAGR for roasting plant and coke oven was 8.3%
231 and 1.2%. In 2015, both emissions from roasting plant and coke oven were 3.5 t, respectively.

232 The slower AAGR of Hg emissions (7.2%) than that of crude steel production (13%)
233 reflected the impact on Hg emission reduction due to energy saving and environmental
234 protection in ISP. On one hand, Hg input to produce unitary crude steel decreased from 0.17
235 to 0.12 g/t, which mainly benefited from the improvement of coke production efficiency and
236 energy utilization efficiency of sinter/pellet plant and blast furnace. Since 2004, indigenous
237 coke production method with high coal consumption has been gradually replaced with
238 machine coke production method. The coke ratio in sinter/pellet plant has been reduced from
239 approximately 388 kg/t pig iron produced in 2000 to 363 kg/t in 2015 (CISIA, 2001-2016).
240 On the other hand, the improvement of APCDs increased the overall Hg removal efficiency
241 from 47% in 2000 to 65% in 2015 (**Fig. 3**). APCDs for coke oven have shown the largest Hg
242 removal efficiencies (64%-87%) while pollution control in sinter/pellet plant contributed most
243 to the rapid Hg reduction speed during 2000-2015. The replacement of CYC and WS with
244 ESP and FF in sinter/pellet plant improved Hg removal efficiency from 21% in 2000 to 44%
245 in 2010. The application of FGD in addition to dust collectors was the main driver of Hg
246 reduction in sinter/pellet process during 2011-2015. Hg removal efficiency in sinter/pellet
247 plant was 53% in 2015.

248 3.2.2 Hg emission trends by province

249 Provincial Hg emissions in 2000, 2005, 2010, and 2015 were shown in **Table 2**. In 2000,
250 Shanxi, Shanghai, Henan, Hebei, and Shandong were the top five largest emitters with
251 emissions larger than 1 t. Emissions from these five provinces contributed to 58% of national
252 Hg emissions. Following these five provinces were Liaoning, Beijing, Gansu, Jiangsu, and
253 Jiangxi. Summation of the emissions from all the above ten provinces were 9.0 t, accounting
254 for 78% of national emissions in 2000. At the provincial level, we noted significant
255 differences of Hg emission trends during the past 16 years. The AAGR of provincial Hg
256 emissions varied from -40% to 26%. Negative AAGR existed in Beijing and Shanghai
257 provinces, the two most economically developed regions in China. Hg abatement in these two
258 regions was mainly caused by the reduction of crude steel production, which was transferred
259 to nearby provinces such as Hebei, Zhejiang, Jiangsu, and Shandong. Thus, Hg emissions in
260 these nearby provinces all presented high AAGR of more than 10%. In 2015, the largest five
261 Hg emission provinces were changed to Hebei, Shandong, Henan, Jiangsu, and Shanxi
262 provinces. Emissions from these provinces reached 21.5 t, accounting for 68% of national
263 emissions. Liaoning, Jiangxi, Inner Mongolia, Gansu, and Shanghai were also in the list of the
264 top ten largest emitters.

265 3.2.3 Hg emission trends by species

266 Overall Hg speciation profile of ISP experienced great change during the study period,
267 from 50/44/6 (gaseous elemental Hg (Hg^0)/gaseous oxidized Hg (Hg^{II})/particulate-bound Hg
268 (Hg_p)) in 2000 to 40/59/1 in 2015 (**Fig. 4**). The proportion of Hg^{II} increased 15%, whereas
269 both Hg^0 and Hg_p proportion showed decreasing trend. Such shift indicated higher deposition
270 proportion of Hg around the emission points since Hg^{II} has larger deposition velocity and
271 higher water-solubility. For the long process steel making, Hg speciation profile shifted from
272 49/44/7 in 2000 to 39/60/1. The speciation shift in roasting plants was mainly impacted by the
273 replacement of WS and CYC with FF, which increased the emitted Hg^{II} proportion from 38%
274 to 75%. The replacement of indigenous coke production method with machine coke
275 production method mainly contributed to Hg^{II} proportion increase from 42% to 52% at first.
276 However, the gradual installation of WS in addition to cooler for air pollution control of

277 machine coke production method further washed Hg^{II} and reduced Hg^{II} proportion to 49% in
278 2015. Hg^{II} proportion in the exhaust gas of sinter/pellet plant has increased by 20%. The
279 increase of Hg^{II} proportion in sinter/pellet plant was mainly impacted by the substitute of WS
280 with ESP, FF, ESP+WFGD, or ESP+DFGD+FF which generally emitted gas with higher Hg^{II}
281 proportion (**Table S4**). Increase of Hg^{II} emission proportion in blast furnace was due to higher
282 Hg^{II} emission proportion after FF than venturi. In the oxygen steel making process, Hg
283 speciation profile almost unchanged. For the short process steel making, Hg^0 was the
284 dominant speciation during the whole study period and the proportion of Hg^0 increased from
285 66% in 2000 to 79% in 2015.

286 **3.3 Uncertainty analysis**

287 In 2015, overall uncertainty of atmospheric Hg emissions from ISP was in the range of
288 (-29%, 77%) (**Fig. 5**). Previous studies in ISP indicated the emission uncertainties of this
289 source were (-80%.100%) in the study of Zhang et al. (2015) and (-100%, 100%) in the study
290 of Streets et al. (2005) and Wu et al. (2006). The improvement of emission estimation of this
291 study was contributed by better knowledge on the Hg concentrations of raw materials and Hg
292 removal efficiencies of APCDs. In all ISP processes, the largest uncertainties existed in
293 emissions from roasting plant (-59%, 130%) and sinter/pellet process (-45%, 126%). These
294 mainly due to larger distribution range of Hg concentrations in limestone and iron ore as well
295 as Hg removal efficiencies of APCDs. The uncertainties of Hg emissions from other processes
296 were much lower, (-49%, 48%) for coke oven, (-23%, 46%) for blast furnace, (-41%, 27%)
297 for oxygen steel making, and (-60%, 54%) for arc steel making.

298 **3.4 Comparison and implications**

299 Due to the complicated ISP processes and limitations of data availability, the process
300 combinations considered in different inventories were divided into four types (**Fig. 6**)
301 (AMAP/UNEP, 2008, 2013; Wang K. et al., 2016; Wu et al., 2016; Wu et al., 2006; Zhang et
302 al., 2015a). The first type included sinter plant and blast furnace, which were the basic
303 assumption in the emission inventories of Wu et al. (2003), Zhang L. et al. (2015), and
304 AMAP/UNEP (2005). In these studies, unique emission factor of 0.0400 g/t was applied

305 (Table S5) and their emissions were similar in the same inventory year. Our emissions for this
306 process combination were almost the same as above estimations around 2005. However, the
307 gap grew with time when FGD was gradually applied in sinter/pellet plant. Therefore,
308 emission factor for this type of combination was reduced from 0.0527 g/t in 2000 to 0.0296
309 g/t in 2015 (Table S5). The second type also consisted of steel making in addition to the first
310 type. Our estimation was much higher than the study of Wang K. et al. (2016) because the
311 emission factors applied in Wang K.'s study were mainly derived from European technical
312 report (EMEP/CORINAIR, 2001; EMEP/EEA, 2013). However, the technology applied in
313 Europe may be better than China's situation. For example, the emission factor of 0.00019 g/t
314 applied for blast furnace with FF was used as best emission factor in Wang K.'s study (2016).
315 However, the combination of WS and venturi scrubber was the dominant APCD type for
316 China's blast furnace (Zhao et al., 2013), Hg removal efficiency of which was lower than that
317 of FF. The third type of process combination also included coke oven as part of ISP in
318 addition to the second type. Lower Hg emissions estimated by AMAP/UNEP (2013) were due
319 to their lower Hg concentration in coal. In addition, although different processes were
320 considered in the global report, unique APCD profile was applied for different process. The
321 application proportion of ESP+FGD reached 55%. However, FGD were mainly installed in
322 sinter/pellet plant but rarely applied in other processes. Thus, the emissions estimated by the
323 global report were lower than our estimation. The fourth type also considered the emissions
324 from roasting process where emissions accounted for 9%-11% of total emissions.

325 The comparison of emissions from different types of process combination in this study
326 indicated the significance of including emissions from roasting plant and coke oven in the ISP
327 emission inventories. The proportion of emissions from these two processes accounted for
328 22%-34% of ISP's emissions during the whole study period. In addition, these two processes
329 were important in shaping the trends of ISP Hg emissions. For example, Hg emissions of all
330 processes showed an increase during 2007-2008 (Red line in Fig. 6). However, if these two
331 processes were not considered, we will observe a decreasing trend (Green and orange line in
332 Fig.6). Moreover, given the impact of APCDs on the emission estimation, inventories in ISP
333 should also apply distinct APCD profiles for different processes so as to reduce the

334 uncertainty of inventories.

335 Future Hg emission for ISP was forecasted to decrease based on comprehensive
336 consideration of dominant parameters (e.g., steel production, air pollution control measures)
337 in the technology-based method and the emission trends from China's ISP during 2000-2015.
338 On one aspect, the annual growth rate of crude steel production reduced from 14.2% of
339 2000-2014 to 1.24% of 2015-2016. Thus, China's ISP has passed the quick growth period.
340 During 2014-2016, the crude steel production was around 810 Mt. It was expected the peak of
341 crude steel production was in the range of 669-1092 Mt (Zhong, 2013) and the crude steel
342 production in 2020 will ranged in 750-800 Mt (MIIT, 2016). Therefore, the peak of crude
343 steel production may have arrived or be coming. And slow decreasing crude steel production
344 was expected after the peak according to the development trends of mineral resources
345 consumption rule in developed countries. In addition, with the coming of high-yield-period of
346 steel scrap production (Guo and Wei, 2010), the application proportion of short process steel
347 making method is expected to increase, which will indirectly reduce the requirement of steel
348 production from long process steel making method. The replacement of steel production
349 method will also be one driver of Hg emission reduction considering lower Hg emission
350 factors of short process. Moreover, energy consumptions are required to be reduced by more
351 than 10% during the 2016-2020 (MIIT, 2016) and energy savings will be a long-term strategic
352 in China. The improvement of energy efficiency in the main processes will reduce energy
353 consumption (Li et al., 2015) and further lead to the reduction of Hg input. On the other
354 aspect, emissions of pollutants (eg., SO₂, NO_x, and PM) are required to be reduced by at least
355 15% for ISP before 2020 in China (MIIT, 2016). To fulfill this goal, corresponding emission
356 standards have been issued (Wu, 2013), which will accelerate the applications of improved
357 APCDs. During 2010-2015, the increase of SO₂ emission limits from 1500 mg/m³ to 200
358 mg/m³ promoted the large-scale application of desulfurization devices in the sinter/pellet plant
359 of ISP. After 2015, ISP will move forward to NO_x control by using related technologies such
360 as selective catalytic reduction (SC, 2013), the synergic Hg removal efficiencies of which
361 have been proved in other industries (Wang et al., 2010). If we assumed that the crude steel
362 production reached a conservative value of 1000 Mt and that advanced dust collectors (ESP or

363 FF), desulfurization towers, and denitration technologies were fully applied in ISP,
364 atmospheric Hg emissions in ISP will be reduced to 27 t in 2020. Thus, a decreasing trend
365 will be expected from 2015 to 2020. Such conclusion is opposite with the study using
366 transformed normal distribution method (Wu et al., 2016). In this study, the transformed
367 normal distribution function was applied to estimate atmospheric Hg emissions from ISP. By
368 using such semi-quantitative method, the emission factor in 2020 (0.0402 g/t for long process
369 and 0.0211 g/t for short process) was almost the same as that in 2015 (0.0403 g/t for long
370 process and 0.0212 g/t for short process). Thus, atmospheric Hg emissions in 2020 will
371 almost depend on crude steel production and the emissions in 2020 will reach 40 t at the
372 conservative situation. Therefore, the technology-based emission factor method will provide
373 more objective forecast of future emissions.

374 **4 Conclusion**

375 In this study, atmospheric Hg emissions from ISP during 2000-2015 were estimated by
376 using technology-based emission factor method with up-to-date parameters. The input of Hg
377 as impurity of raw materials of ISP increased from 21.6 t in 2000 to 94.5 t in 2015. In the
378 various types of raw materials, coking coal and iron concentrates contributed to the largest
379 amount of Hg input, 35%-46% and 25%-31% of national total, respectively. Atmospheric Hg
380 emissions from ISP increased from 11.5 t in 2000 to the peak of 35.6 t in 2013, and then
381 reduced to 32.7 t in 2015. Overall Hg speciation shift from 50/44/6 ($\text{Hg}^0/\text{Hg}^{\text{II}}/\text{Hg}_p$) in 2000 to
382 40/59/1 in 2015. In the coming years, emissions from ISP are expected to decrease due to the
383 projection of Hg input reduction and improvement of APCDs.

384 In 2015, emissions from long process steel making method and short process steel
385 making were 32.2 t and 0.5 t, accounting for 98.3% and 1.7% of national total, respectively.
386 Sinter/pellet plant and blast furnace were the largest two emission processes, accounted for 49%
387 and 24% of national emissions, respectively. However, emissions from roasting and coke
388 oven should cause attention because their emissions accounted for 22% of national emissions.
389 The largest five Hg emission provinces were Hebei, Shandong, Henan, Jiangsu, and Shanxi
390 provinces. Emissions from these provinces reached 21.5 t, accounting for 68% of national
391 emissions.

392 In this study, we applied the technology-based emission factor method for better
393 quantification of Hg into ISP and atmospheric Hg emissions from different processes of ISP.
394 Compared with previous studies, the uncertainty of atmospheric Hg emissions from ISP has
395 largely reduced with better understanding of Hg flow in ISP. This method has provided more
396 objective estimation of current emissions and forecast of future emissions. However, with the
397 continuously change of APCD combinations, extensive and dedicated field experiments are
398 still required to generate suitable database of Hg removal efficiencies for the improved
399 APCDs in the future.

400 *Acknowledgment.* This study was supported by the Major State Basic Research Development
401 Program of China (973 Program) (2013CB430001), Natural Science Foundation of China
402 (21607090), and China Postdoctoral Science Foundation (2016T90103, 2016M601053)

403

404 **References**

- 405 Arctic Monitoring and Assessment Programme and United Nations Environment Programme
406 (AMAP/UNEP): Technical background report to the global atmospheric mercury
407 assessment, AMAP/UNEP, Geneva, Switzerland, 2008.
- 408 Arctic Monitoring and Assessment Programme and United Nations Environment Programme
409 (AMAP/UNEP): Technical background report for the global mercury assessment,
410 AMAP/UNEP, Geneva, Switzerland, 2013.
- 411 China Iron and Steel Industry Association (CISIA): China Steel yearbook, CISIA, Beijing,
412 China, 2001-2016.
- 413 European Monitoring and Evaluation Programme/Core Inventory of Air Emissions Project
414 (EMEP/CORINAIR): Emission inventory guidebook, EMEP/CORINAIR, Copenhagen,
415 Denmark, 2001.
- 416 European Monitoring and Evaluation Programme/European Economic Area (EMEP/EEA):
417 Air pollutant emission inventory guidebook 2013, EMEP/EEA, Copenhagen, Denmark,
418 2013.
- 419 Gao, W.: Study on atmospheric mercury emission characteristics for iron and steel producing
420 process in China, Tsinghua University, School of Environment, Beijing, China, 2016.
- 421 Guo, T., and Wei, L.: Development direction of the recycling industry of secondary zinc
422 resources, China Nonfer. Metal., 4, 2010.
- 423 Hui, M. L., Wu, Q. R., Wang, S. X., Liang, S., Zhang, L., Wang, F. Y., Lenzen, M., Wang, Y.
424 F., Xu, L. X., Lin, Z. T., Yang, H., Lin, Y., Larssen, T., Xu, M., and Hao, J. M.: Mercury
425 Flows in China and global drivers, Environ. Sci. Technol., 51, 222-231, 2016.
- 426 Li, X. C., Gao, X., and Jiang, X. D.: Analysis on potential of energy conservation of Chinese
427 steel industry in the 13th five-year period, The tenth annual conference of China steel
428 and the sixth annual academic conference of Baogang, Shanghai, Beijing, 2015-10-21,
429 2015.
- 430 Liu, H., Fu, M. L., Jin, X. X., Shang, Y., Shindell, D., Faluvegi, G., Shindell, C., and He, K.
431 B.: Health and climate impacts of ocean-going vessels in East Asia, Nature climate
432 change, 6, 1037-1041, 2016.
- 433 Ma, H. L.: China steel statistics, Development and Planning Division of Ministry of
434 Metallurgical, Beijing, China, 1995.
- 435 Ma, J.: Review and projection of technology development of lime used in China's steel
436 industry, China steel, 6, 17-20, 2011.
- 437 Ministry of Environmental Protection (MEP): "Twelfth Five-year" plan for the comprehensive
438 prevention and control of heavy metal pollution, MEP, Beijing, China, 2011.
- 439 Ministry of industry and information Technology (MIIT): Adjustment and upgrading plan of
440 iron and steel industry (2016-2020), MIIT, Beijing, China, 2016.
- 441 National Statistical Bureau of China (NBS): China Environmental Statistics Yearbook, NBS,
442 Beijing, China, 2001-2016.
- 443 National Energy Administration (NEA): Action plan of coal clean utilization, NEA, Beijing,
444 China, 2014.
- 445 National Energy Statistical Agency of China (NESAC): China Energy Statistical Yearbook,
446 NESAC, Beijing, China, 2001-2016.

447 State Council of the People's Republic of China (SC): Action plan of national air pollution
448 prevention and control, SC, Beijing, China, 2013.

449 Streets, D. G., Hao, J. M., Wu, Y., Jiang, J. K., Chan, M., Tian, H. Z., and Feng, X. B.:
450 Anthropogenic mercury emissions in China, *Atmos. Environ.*, 39, 7789-7806, 2005.

451 Swaine, D. J.: Environmental aspects of trace-elements in coal, *Environ. Geochem. Health*, 14,
452 2-2, 1992.

453 Tao, S. R., and Wang, Y. J.: Impact on the economic benefits of metallurgy industry from
454 coke coal quality, *Coal Proc. Compre. Utiliz.*, 4, 1994.

455 Tian, H. Z., Wang, Y., Xue, Z. G., Cheng, K., Qu, Y. P., Chai, F. H., and Hao, J. M.: Trend and
456 characteristics of atmospheric emissions of Hg, As, and Se from coal combustion in
457 China, 1980-2007, *Atmos. Chem. Phys.*, 10, 11905-11919, 2010.

458 Tian, H. Z., Zhu, C. Y., Gao, J. J., Cheng, K., Hao, J. M., Wang, K., Hua, S. B., Wang, Y., and
459 Zhou, J. R.: Quantitative assessment of atmospheric emissions of toxic heavy metals
460 from anthropogenic sources in China: historical trend, spatial distribution, uncertainties,
461 and control policies, *Atmos. Chem. Phys.*, 15, 10127-10147, 2015.

462 United Nations Environment Programme (UNEP): Toolkit for identification and
463 quantification of mercury releases. Guideline for inventory level 2, version 1.3. , 2013.

464 United States Environmental Protection Agency (US EPA): Method 7473: Hg in solids and
465 solutions by thermal decomposition amalgamation and atomic absorption
466 spectrophotometry, US EPA, Washinton D. C., United States, 1998.

467 United States Geological Survey (USGS): Mercury content in coal mines in China, Reston,
468 Virginia, United States, 2004.

469 Wang, F. Y., Wang, S. X., Zhang, L., Yang, H., Gao, W., Wu, Q. R., and Hao, J. M.: Mercury
470 mass flow in iron and steel production process and its implications for mercury emission
471 control, *J. Environ. Sci.*, 43, 293-301, 2016.

472 Wang, K., Tian, H. Z., Hua, S. B., Zhu, C. Y., Gao, J. J., Xue, Y. F., Hao, J. M., Wang, Y., and
473 Zhou, J. R.: A comprehensive emission inventory of multiple air pollutants from iron and
474 steel industry in China: Temporal trends and spatial variation characteristics, *Sci. Total*
475 *Environ.*, 559, 7-14, 2016.

476 Wang, S. X., Zhang, L., Li, G. H., Wu, Y., Hao, J. M., Pirrone, N., Sprovieri, F., and Ancora,
477 M. P.: Mercury emission and speciation of coal-fired power plants in China, *Atmos.*
478 *Chem. Phys.*, 10, 1183-1192, 2010.

479 Wang, S. X., Zhao, B., Cai, S. Y., Klimont, Z., Nielsen, C. P., Morikawa, T., Woo, J. H., Kim,
480 Y., Fu, X., Xu, J. Y., Hao, J. M., and He, K. B.: Emission trends and mitigation options
481 for air pollutants in East Asia, *Atmos. Chem. Phys.*, 14, 6571-6603, 2014.

482 Wang, Y. F.: Analysis on the harm of indigenous coking, *Coal Eco. Res.*, 1, 1991.

483 Wu, Q. R., Wang, S. X., Zhang, L., Song, J. X., Yang, H., and Meng, Y.: Update of mercury
484 emissions from China's primary zinc, lead and copper smelters, 2000-2010, *Atmos.*
485 *Chem. Phys.*, 12, 11153-11163, 2012.

486 Wu, Q. R., Wang, S. X., Li, G. L., Liang, S., Lin, C.-J., Wang, Y. F., Cai, S. Y., Liu, K. Y., and
487 Hao, J. M.: Temporal trend and spatial distribution of speciated atmospheric mercury
488 emissions in China during 1978–2014, *Environ. Sci. Technol.*, 50, 13428-13435, 2016.

489 Wu, S. H.: Interpretation about “Emission Standards of Iron and Steel Industrial Pollutants”,
490 *Indus. Safety Environ. Pro.*, 29, 2, 2013.

491 Wu, Y., Wang, S. X., Streets, D. G., Hao, J. M., Chan, M., and Jiang, J. K.: Trends in
492 anthropogenic mercury emissions in China from 1995 to 2003, *Environ. Sci. Technol.*, 40,
493 5312-5318, 2006.

494 Zhang, L.: Emission characteristics and synergistic control strategies of atmospheric mercury
495 from coal combustion in China, Ph.D. Dissertation, Tsinghua University, School of
496 Environment, Beijing, China, 2012.

497 Zhang, L., Wang, S. X., Meng, Y., and Hao, J. M.: Influence of mercury and chlorine content
498 of coal on mercury emissions from coal-fired power plants in China, *Environ. Sci.*
499 *Technol.*, 46, 6385-6392, 2012.

500 Zhang, L., Wang, S. X., Wang, L., Wu, Y., Duan, L., Wu, Q. R., Wang, F. Y., Yang, M., Yang,
501 H., Hao, J. M., and Liu, X.: Updated emission inventories for speciated atmospheric
502 mercury from anthropogenic sources in China, *Environ. Sci. Technol.*, 49, 3185-3194,
503 2015a.

504 Zhang, Y. H., Zhang, C., Wang, D. Y., Luo, C., Yang, X., and Xu, F.: Characteristic of
505 mercury emissions and mass balance of the typical iron and steel industry, *Environ. Sci.*,
506 36, 8, 2015b.

507 Zhao, B., Wang, S. X., Liu, H., Xu, J. Y., Fu, K., Klimont, Z., Hao, J. M., He, K. B., Cofala, J.,
508 and Amann, M.: NO_x emissions in China: historical trends and future perspectives,
509 *Atmos. Chem. Phys.*, 13, 9869-9897, 2013.

510 Zhong, X. G.: Research on historical development and market forecast of China 's crude steel
511 production, *Indus. Econo.*, 32-33, 2013.

512

513 **Tables**

514 Table 1. Hg concentration in the raw materials

Province ¹	Iron ore				Limestone				Dolomite				Coking coal				PCI coal			
	AM ²	MV ²	SD ²	NS ²	AM	MV	SD	NS	AM	MV	SD	NS	AM	MV	SD	NS	AM	MV	SD	NS
	ng/g	ng/g	ng/g		ng/g	ng/g	ng/g		ng/g	ng/g	ng/g		ng/g	ng/g	ng/g		ng/g	ng/g	ng/g	
Tianjin	41	44	8	3	9	9		1	5	5	2	4					75	66	31	5
Hebei	37	24	40	79	374	117	631	27	7	8	5	5	78	66	39	71	79	85	70	38
Shanxi	30	24	28	25	9	7	8	6					77	71	27	22	114	106	19	3
Shanghai	44	44	50	4	20	20		1	39	39	2	2	125	152	71	5	12	12	0	2
Jiangsu					103	68	113	18												
Zhejiang					52	37	35	22												
Anhui	21	20	12	14	11	11	4	12	32	32	2	3	88	58	53	8	98	22	104	7
Fujian	19	14	11	15	11	11	5	4	9	8	5	4	105	100	51	13	255	239	51	7
Jiangxi	57	46	88	18					10	9	4	3	120	93	59	4	185	198	66	7
Shandong	125	128	73	20					24	24	1	2	72	69	21	12				
Henan	32	24	29	18	692	759	629	13												
Hubei					16	14	8	6					92	83	54	39	131	116	91	21
Hunan	33	19	34	77	102	87	62	4	3	3	1	2								
Guangdong					48	44	26	15												
Guangxi					8	8	2	4					210	188	112	27	96	98	30	6
Chongqing													85	79	48	20	65	65	12	4
Sichuan	37	2	44	7	10	9	4	12												
Guizhou					11	10	11	42												
Yunnan	10	10	7	6	17	20	7	6					51	52	7	8	58	56	6	3

Gansu	107	107	3	3	3	3		1					166	174	21	5	60	60	5	2
Xinjiang	6	5	4	17									82	82	46	22	31	24	19	15
National	38	20	48	306	153	18	402	204	14	9	12	25	99	82	68	256	99	73	83	120

515 Note: 1. Provinces without data were not listed in this table;

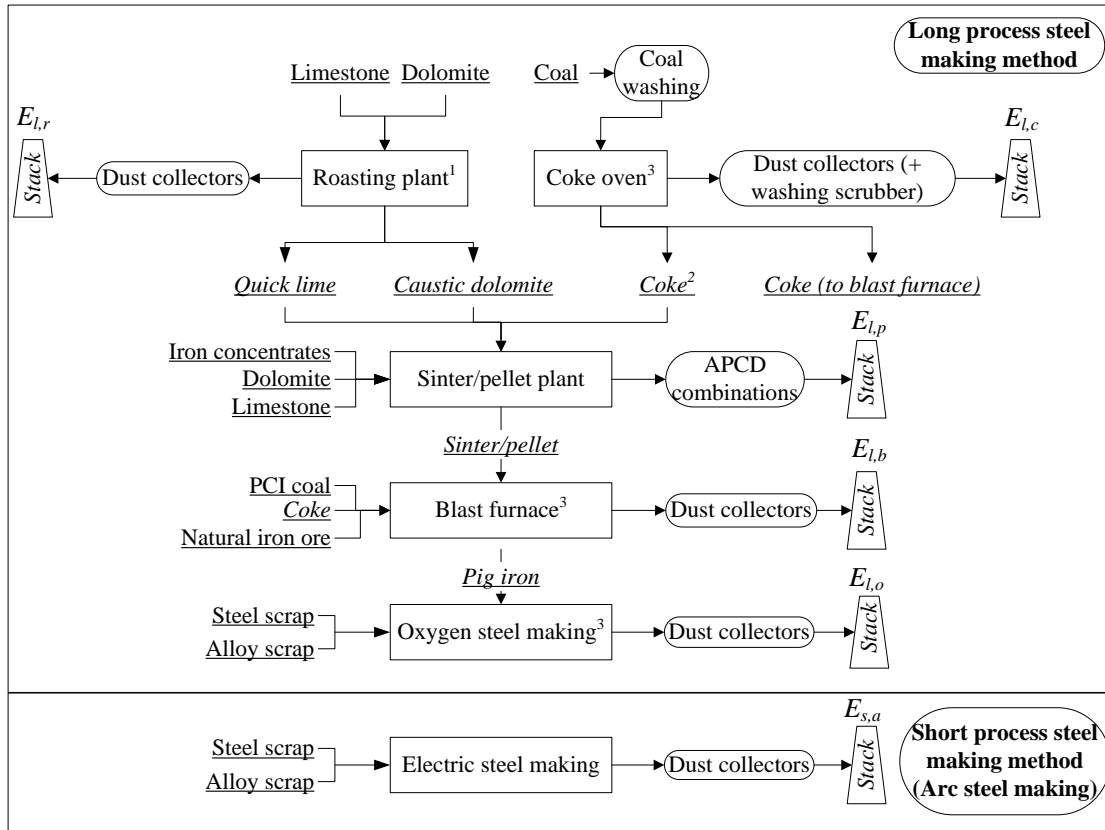
516 2. AM: Average mean; MV: Median value; SD: Standard deviation ; NS: Number of samples;

517 -.

518 Table 2. Provincial Hg emissions during 2000-2015

Province ¹	Atmospheric Hg emissions (kg)				
	2000	2005	2010	2015	AAGR
Beijing	432.0	316.1	132.9	0.0	-40%
Tianjin	260.0	482.0	863.4	688.9	7%
Hebei	1202.0	4016.0	6672.3	7129.3	13%
Shanxi	1587.3	2214.2	2075.2	1792.3	1%
Inner	287.5	477.8	667.7	753.8	7%
Liaoning	845.8	1171.1	1679.3	1563.4	4%
Jilin	109.5	190.9	282.8	267.9	6%
Heilongjiang	71.4	171.4	307.3	180.2	6%
Shanghai	1532.6	1155.7	1021.2	703.6	-5%
Jiangsu	304.5	1149.5	1891.4	2519.4	15%
Zhejiang	75.9	139.8	356.2	362.0	11%
Anhui	252.5	399.4	572.6	586.6	6%
Fujian	67.9	150.2	243.8	309.2	11%
Jiangxi	292.1	701.4	1054.0	984.8	8%
Shandong	1122.5	3965.4	6017.7	6051.1	12%
Henan	1259.8	2172.9	3495.3	4049.9	8%
Hubei	268.0	363.7	467.6	376.7	2%
Hunan	239.2	512.1	713.7	627.2	7%
Guangdong	131.7	286.6	339.7	395.9	8%
Guangxi	82.4	236.8	423.6	538.9	13%
Hainan	0.1	0.5	0.0	3.1	26%
Chongqing	106.2	121.7	168.4	142.3	2%
Sichuan	224.6	353.7	400.2	377.5	4%
Guizhou	100.9	235.4	204.1	187.4	4%
Yunnan	99.0	299.4	382.9	283.0	7%
Shaanxi	75.8	222.7	395.9	689.5	16%
Gansu	372.5	528.5	612.8	708.1	4%
Qinghai	12.2	10.6	64.5	24.8	5%
Ningxia	10.0	28.9	72.6	139.8	19%
Xinjiang	50.1	97.0	286.8	294.6	13%
Total	11476	22171	31866	32732	7%

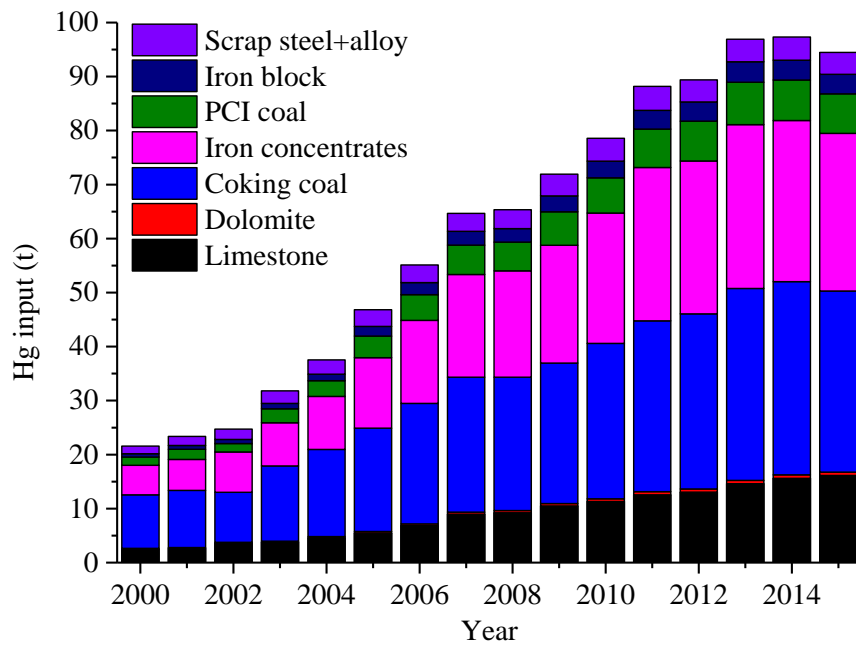
519 Note: 1. Provinces without data were not listed in this table.



Note: 1. Some plants roasted limestone and dolomite separately.
 2. Mainly coke breeze. Some plants also use coal powder as fuel.
 3. The flue gas after dust collectors are collected in gasometer before use.

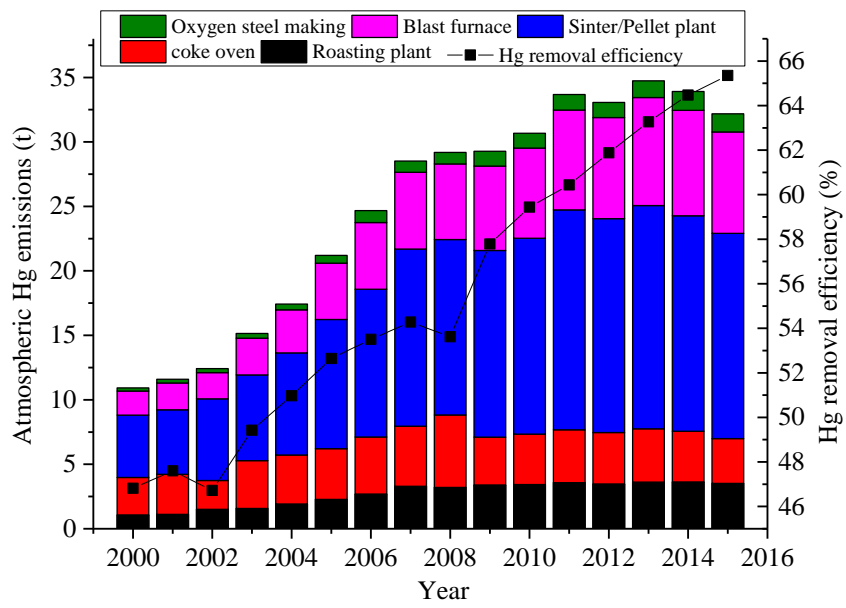
521

522 **Fig. 1.** Flow chart of ISP processes



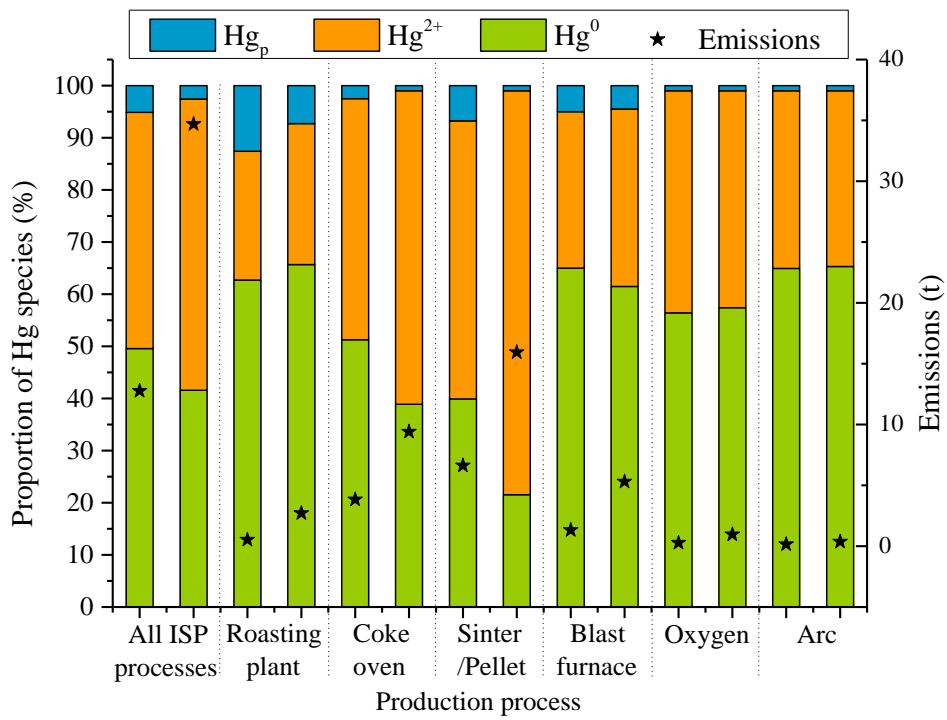
523

524 **Fig. 2.** Hg input trends by material



525

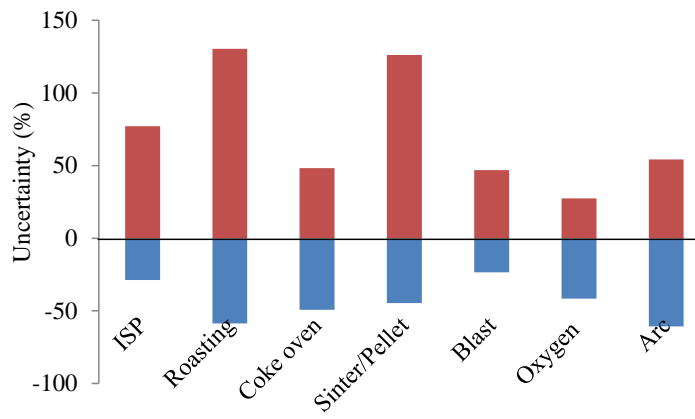
526 **Fig. 3.** Hg emission trends by process and Hg removal efficiency



527

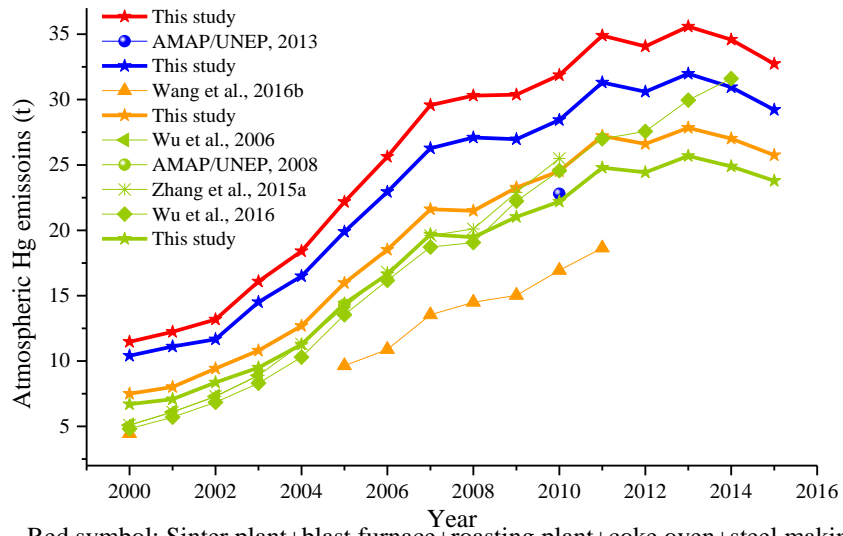
528 **Fig. 4.** Proportion of different Hg species (For each process, the left and right column

529 represents the data in 2000 and 2015, respectively)



530

531 **Fig. 5.** Unertainty analysis



Red symbol: Sinter plant+blast furnace+roasting plant+coke oven+steel making
 Blue symbol: Sinter plant+blast furnace+coke oven+steel making
 Orange symbol: Sinter plant+blast furnace+steel making
 Green symbol: Sinter plant+blast furnace

532

533 **Fig. 6.** Atmospheric Hg emissions of ISP in different studies

534